INTERNATIONAL JOURNAL OF SUSTAINABLE ENERGY
2022, VOL. 41, NO. 5, 469–491
https://doi.org/10.1080/14786451.2021.1953495

Taylor & Francis
Taylor & Francis Group

Structural optimisation framework for onshore wind turbine towers considering multiple design constraints

Shaikha Al-Sanad[a], Jafarali Parol[a], Lin Wang[b] and Athanasios Kolios [c]

[a]Energy and Building Research Center, Kuwait Institute for Scientific Research, Safat, Kuwait; [b]School of Mechanical, Aerospace and Automotive Engineering, Coventry University, Coventry, UK; [c]Department of Naval Architecture, Ocean and Marine Engineering, University of Strathclyde, Glasgow, UK

ABSTRACT

An optimum design of the onshore wind turbine (WT) tower structure is crucial for achieving an economic, efficient and safe design of the entire onshore WT system. In this study, an integrated structural optimisation framework for onshore WT towers is established through combining a parametric finite element analysis (FEA) model with a genetic algorithm (GA). The bottom and top diameters as well as the thickness distribution of the onshore WT tower are considered as design variables. The mass of the onshore WT tower is minimised by the structural optimisation framework under multiple design constraints. The framework has been validated and then applied to the structural optimisation of a representative 2.0 MW onshore WT tower presently installed in a wind farm in Middle East. It is demonstrated that the structural optimisation framework developed in this work can considerably lower the mass of the tower while fulfilling design requirements.

ARTICLE HISTORY
Received 30 June 2021
Accepted 4 July 2021

KEYWORDS
Onshore wind turbines; wind turbine tower; structural optimisation framework; finite element analysis; genetic algorithm

1. Introduction

As a renewable and clean energy resource, wind energy is capable of battling both the energy crisis and global warming. Many countries, such as the UK and China, have made significant efforts in the development of wind farms to harvest the wind energy. By the end of 2018, the cumulatively installed capacity of wind turbines (WTs) worldwide reached 591 GW, supplying around 6% of the global electricity demand (Ohlenforst et al. 2019). Projections have shown that globally installed wind power capacity will reach 2110 GW by the end of 2030, which reduces the annual emissions of CO_2 by over 3.3 billion tonnes (Fried et al. 2016) and creates around 2.4 million new jobs.

WT tower elevates rotor blades to a specific height for accessing desirable wind shear and supports the major components of the WT, such as the rotor and the nacelle. The overall performance and structural responses of the WT can be significantly affected by the tower structural properties, such as the tower's natural frequency and stiffness. Inappropriate design of WT towers may lead to resonance, buckling and inadequate strength to withstand wind-induced loads. Moreover, the cost of the tower constitutes approximately 14~20% of the overall capital cost of an onshore WT (Stehly et al. 2018). Hence, to ensure an economic, efficient and safe design of the entire onshore WT system, it is crucial to have an optimum design of the WT tower structure, meeting all design constraints (e.g. fatigue, buckling and vibration, etc.) and having a minimum mass (cost).

Two main components are required in a structural optimisation framework of onshore WT towers, i.e. (1) a structural model for onshore WT towers, which calculates the structural response

CONTACT Lin Wang ac7966@coventry.ac.uk

of the tower, e.g. deformations, stress distributions, vibration shapes, etc.; and (2) an optimisation algorithm, which searches for optimum solutions under multiple design constraints.

There are two main types of structural models for onshore WT towers, i.e. (1) beam model, in which the tower structure is discretised into beam elements; and (2) finite element analysis (FEA) model, which constructs the tower structure using 3D brick or shell elements. Because of its computational efficiency, the beam model has been extensively employed for structural modelling of onshore WT towers (Murtagh, Basu, and Broderick 2004) and blades (Wang et al. 2014). Although efficient, it is incapable of precisely capturing local structural responses, e.g. stress concentration effects (Petrini et al. 2010). To accurately predict structural responses, it is necessary to model a WT tower utilising the 3D FEA, which is capable of providing accurate results and examining detailed stress distributions. Because of its high fidelity, the 3D FEA model has been increasingly utilised for structural modelling of WT structures (Martinez-Luengo, Kolios, and Wang 2017; Wang, Quant, and Kolios 2016b; Kolios et al. 2019). Thus, the 3D FEA model is selected in this work to capture structural responses of WT towers.

Optimisation algorithms can be roughly classified into three types, i.e. (1) exact algorithms, in which all possible combination of design variables are evaluated to find the best solution; (2) heuristic algorithms, which employ semi-empirical rules to search for near-optimum solutions; and (3) metaheuristic algorithms, which are intelligently problem-independent algorithms to search for near-optimum solutions. Exact algorithms are precise, as every possible solution is evaluated. However, in cases of a large number of design variables, the evaluation of every possible combinations requires tremendous computational resources, making the exact algorithms extremely time-consuming and even infeasible. In comparison to exact algorithms, the heuristic algorithms require less computational resources. However, their accuracy is greatly dependent on the precision of semi-empirical rules and they are problem-dependent, which limit their applications to a certain extent. Metaheuristic algorithms are problem-independent, and they are generally developed on the basis of the optimisation processes observed in nature, e.g. ant colony optimisation (ACO) (Angus and Woodward 2009), elephants herding optimisation (Riffi 2020), and genetic algorithm (GA) (Kramer 2017), etc. Among them, the GA, which finds the optimum solution based on the process inspired by Darwin's theory of natural selection, is capable of finding global optima and handling a large number of design variables, making it the most commonly used metaheuristic algorithm (Wang, Kolios, et al. 2016; Gentils, Wang, and Kolios 2017; Joshi, Sandhu, and Bansal 2013; Mellit 2008; Kituu et al. 2012). Thus, the GA is chosen to find the optimum solution in this study.

This paper develops an integrated structural optimisation framework for onshore WT towers, with the consideration of multiple design constraints, through combining FEA with GA. Based on the finite element method, a parametric FEA model of a typical onshore WT tower is established and then validated accordingly through a case study. After the validation, the parametric FEA model is combined with GA to develop a structural optimisation framework for onshore WT towers. The optimisation framework is applied to a representative 2.0 MW onshore WT to reduce the mass of its 78 m-tall tower structure.

The structure of the paper is as follows. Section 2 illustrates the reference model used in this study. Section 3 illustrates the wind conditions and design loads. Sections 4 and 5 present the parametric FEA model of onshore WT towers and the GA, respectively, which are then integrated to establish the structural optimisation framework in Section 6. Section 7 presents results and discussion, and Section 8 presents conclusions.

2. Reference model: 2.0 MW onshore WT with a 78 m-height tower

The reference WT model used in this study is a representative 2.0 MW onshore WT, of which tower height is 78 m. The 2.0 MW onshore WT model is also used in Al-Sanad et al. (2021), in which the tower structure is optimised through a reliability-based design optimisation

Table 1. Main parameters of the reference WT model (Al-Sanad et al. 2021).

Parameters	Value	Unit
Rated power	2.0	MW
Diameter of the rotor	97	m
Number of blades	3	–
Rated rotor speed	19	rpm
Rotor and nacelle assembly (RNA) mass	114,000	kg
Diameter of the tower base	4.5	m
Thickness of the tower base	0.032	m
Diameter of the tower top	2.332	m
Thickness of the tower top	0.023	m
Tower height	78	m
Tower mass	199	ton

framework. Table 1 and Figure 1 present the main parameters and the layout of the reference WT model, respectively.

3. Wind conditions and design loads

3.1. Wind conditions

The WT investigated in this study is currently installed in a wind farm located in Middle East. The wind speed data at the deployment site were measured, and the measured wind speed distribution in 2017 is presented in Figure 2. From Figure 2, we can see that the mean annual wind speed is approximately 8.5 m/s. According to IEC 61400–1 (IEC 2005), this belongs to the II wind class, and the corresponding 50-year extreme wind speed is 59.5 m/s. The mean annual wind speed and the 50-year extreme wind speed at this site are summarised in Table 2. Additional information associated with the wind farm is neglected for confidentiality reasons.

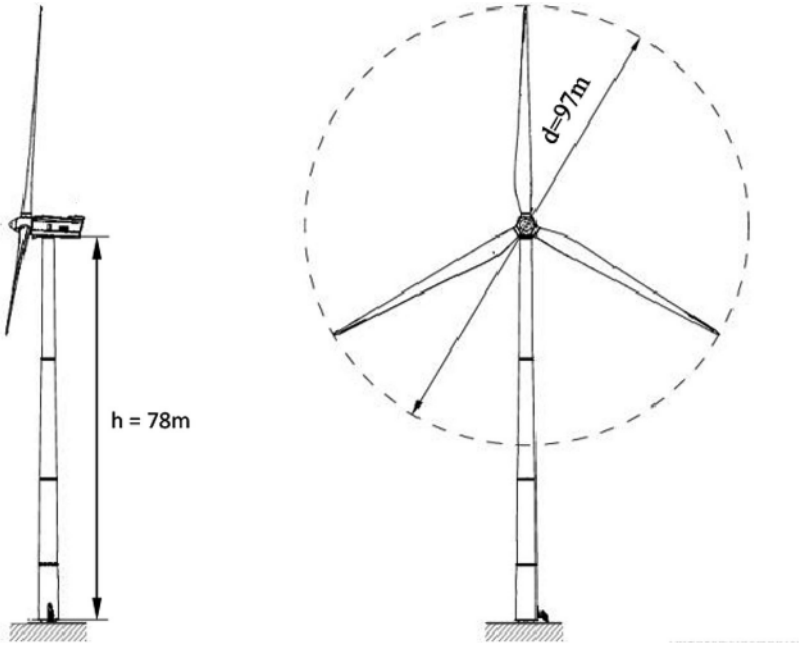

Figure 1. Layout of the reference WT model (Al-Sanad et al. 2021).

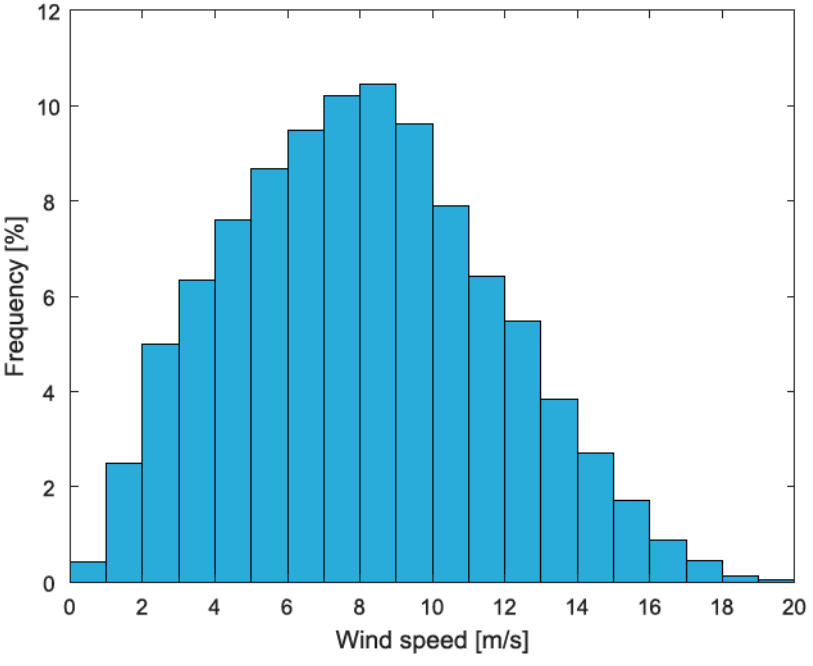

Figure 2. Wind speed distribution measured at the deployment site in 2017 (Al-Sanad et al. 2021).

3.2. Sources of loading

The loads on the onshore WT tower are induced from three sources (Al-Sanad et al. 2021), i.e. (1) aerodynamic loading transferred from rotor blades; (2) wind loading acting on the tower itself; and (3) gravitational loads, which are illustrated in Figure 3.

The loads presented in Figure 3 are detailed below.

3.2.1. Aerodynamic loading transferred from rotor blades

The rotor aerodynamic loading can be transferred to the top of the tower. For instance, the rotor thrust force under extreme wind condition can be calculated by:

$$T = \frac{1}{2}\rho V_{e50}^2 C_T \pi R^2 \tag{1}$$

where ρ is the density of the air having a typical value of 1.225 kg/m^3; V_{e50} represents the extreme wind speed in 50-year return period; C_T is the thrust coefficient; R is the rotor radius.

3.2.2. Wind loading acting on the towerT

When passing the WT, the wind will exert loads on the tower, which can be expressed as:

$$F_{\text{tower}}(z) = \frac{1}{2}\rho C_d D(z) V(z)^2 \tag{2}$$

where $F_{\text{tower}}(z)$ is the wind load acting on the tower segment at height z; C_d is the drag coefficient, of

Table 2. Wind conditions at the deployment site (Al-Sanad et al. 2021).

Item	Value	Unit
Mean annual wind speed	8.5	m/s
50-year extreme wind speed	59.5	m/s

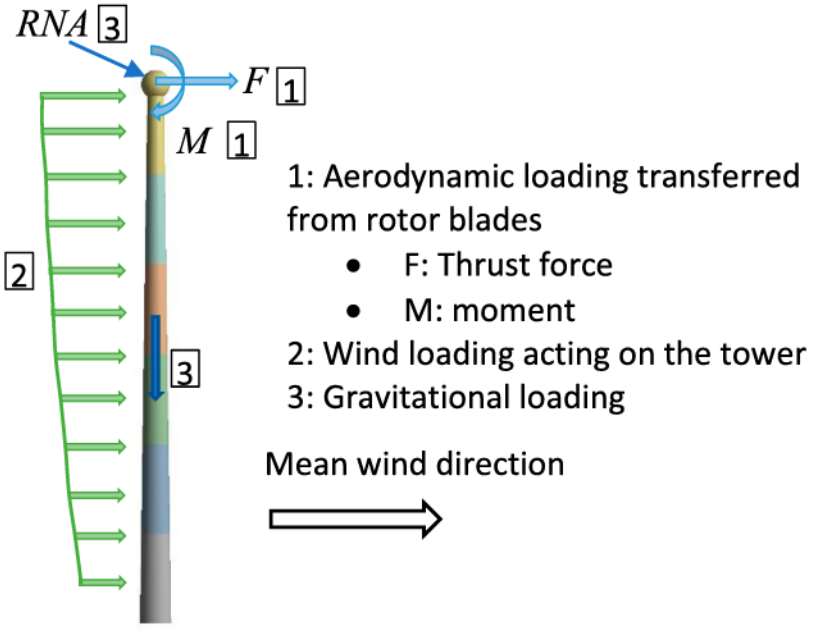

Figure 3. Loads acting on the onshore WT tower.

which value is 0.7 taken from IEC (2005); $D(z)$ and $V(z)$ are the external diameter of tower section and the wind velocity at height z, respectively.

The wind velocity changes with the height because of t wind shear. $V(z)$ in Equation (2) is given by:

$$V(z) = V_{\text{hub}}\left(\frac{z}{z_{\text{hub}}}\right)^{\alpha} \tag{3}$$

where V_{hub} is the wind speed at the height of the hub centre; z and z_{hub} are the height above the ground and the height of the hub centre, respectively; α is the wind shear exponent, of which the typical value is 0.2.

3.2.3. Gravitational loading

The gravitational loads, induced by the weight of the WT tower and the RNA weight at the tower top, can cause the compressive loads on the WT tower and significantly influence the modal frequencies of the tower. Therefore, they should be considered when designing WT towers.

3.3. Load cases

Twenty-two load cases are defined in IEC 61400–1 (IEC 2005) or the design of onshore WTs. These load cases cover every possible operational conditions of an onshore WT, e.g. rump up, emergence stop, normal operation, extreme wind condition, etc. According to the analysis type, these twenty-two load cases can be roughly categorised into two groups, i.e. fatigue and ultimate strength related. For simplicity, the fatigue load under normal operation (Schubel and Crossley 2012) and the ultimate load under the extreme wind conditions with a return period of 50 years (Bir and Migliore 2004; Cox and Echtermeyer 2012) are the typical load cases used in the structural design of onshore WTs.

Both fatigue and ultimate load cases are taken into account in this work. The wind fatigue loads for onshore WTs under normal wind condition are taken into account in the fatigue load case. The extreme wind loads for onshore WTs in the condition of 50-year extreme wind speed are considered in the ultimate load case. Tables 3 and 4 present the fatigue and ultimate aerodynamic loads supplied by the manufacturer of the tower, and these loads are also used in Al-Sanad et al. (2021). The Damage Equivalent Load (DEL) approach, of which further details can be acquired in Freebury and Musial (2000), was used to obtain the fatigue loads in Table 3. The load safety factors for fatigue and ultimate loads are taken as 1.0 and 1.35, respectively, as suggested by IEC 61400–1 (IEC 2005). Table 3 also presents the factored values of ultimate aerodynamic loads.

4. Parametric FEA model of onshore WT towers with shell elements

4.1. Description of the model

A parametric FEA model of onshore WT towers with solid elements has been developed in Al-Sanad et al. (2021). In this study, in order to save computational time, the WT tower will modelled using shell elements, which requires less computational resources than the solid elements. A parametric FEA model of a typical onshore WT tower with shell elements is developed in this study using ANSYS, a commonly used multipurpose FEA software. The flowchart of the model is presented in Figure 4. Each step in the flowchart in Figure 4 is illustrated through the application of the parametric FEA model to the 2.0MW onshore WT tower.

4.2. Application of the parametric FEA model to the 2.0 MW, 78 m onshore WT tower

4.2.1. Defining parameters

In this step, the design parameters that are required in the FEA modelling of onshore WT towers, i.e. the tower thicknesses and diameters data, are defined. These parameters should be linked to the variables of the optimisation problem that will be defined later.

4.2.2. Creating geometric model

The geometric model of the 2.0 MW onshore WT tower is created on the basis of the geometric dimensions presented in Table 1 of Section 2, and it is illustrated in Figure 5. The outer surface of the tower is created in the geometric model. In this step, apart from the external characteristics, additional design considerations are made, such as the division of the tower in sections of common thickness.

4.2.3. Assigning material properties

The tower is fabricated using standard steel S355 grade, a commonly used material for onshore WT towers. Table 5 presents the material properties of S335. It should be notice that the tower thickness data does not cover flanges, paint and bolts. To account for those, the density of the steel is escalated to a value of 8500 kg/m^3, which is 8% higher than the typical value of 7850 kg/m^3.

4.2.4. Generating mesh with shell elements

A structured mesh method is used to generate the mesh for the tower. The shell element Shell281, which is an eight-node element with six degrees of freedom, is used. The details of the shell element

Table 3. Ultimate aerodynamic loads (Al-Sanad et al. 2021).

Items	Unfactored value	Factored value (load safety factor = 1.35)	Unit
$F_{x,u}$	529	714	kN
$M_{y,u}$	5251	7089	kN-m

Note: subscript u denotes ultimate loads.

Table 4. Fatigue aerodynamic loads (load safety factor = 1.0) (Al-Sanad et al. 2021).

Item	Values	Unit
$F_{x,f}$	79	kN
$M_{y,f}$	782	kN-m

Note: subscript f denotes fatigue loads.

Shell281 can be found in ANSYS (2015). A mesh convergence study is performed to determine the proper mesh size. Six mesh sizes are considered, i.e. 2.5, 2, 1.5, 1, 0.5 and 0.25 m. In this case, the tower bottom is fixed and the tower top is loaded with a thrust force of 100 kN. The meshing parameters and calculated maximum deformation are presented in Table 6 and Figure 6.

As can be observed from Table 6 and Figure 6, the maximum deformation reaches convergence at a mesh size of 0.5 m. Further refining the mesh to a size of 0.25 m only yields a relative difference of 0.8%. Thus, 0.5 m is considered as the proper mesh size. Figure 7 depicts the generated mesh for the tower, and the total number of elements is 4368.

4.2.5. Applying loads and defining boundary conditions

For static and fatigue analyses the aerodynamic loads presented in Tables 3 and 4 are, respectively, applied to the top of the WT tower as concentrated loads. The RNA mass is represented by a point mass at the WT tower top. For the ultimate strength load case, the wind loads induced by the wind flowing through the WT tower are considered as distributed loads. It should be noticed that the tower bottom is connected with the foundation in the realistic scenario. However, due to the lack of foundation data for the wind turbine studied in this work, the foundation is not considered in this study. For simplicity, the bottom of the tower is fixed to restrict its movement in this study.

4.2.6. Solving and post-processing results

After the geometry, material, mesh and boundary conditions are defined, different types of analyses (such as buckling and fatigue analyses) can be carried out. The post-processing tools of ANSYS software are then used to plot the FEA simulation results, e.g. stress distributions, deformations, modal shapes, etc.

4.3. Validation of the parametric FEA model with shell elements

To validate the parametric FEA model of onshore WT towers with shell elements that were developed in the previous steps, a case study is carried out. The NREL 5MW WT (Jonkman et al. 2009), which is developed by National Renewable Energy Laboratory (NREL) and a representative MW-scale WT, is taken as an example. Table 7 summarises the geometric and material properties of NREL 5MW WT tower.

The parametric FEA model developed in this work is applied to the NREL 5MW WT tower to compute its natural frequencies of the first two side-to-side and fore-aft modes. In this case, the RNA mass is applied to the top of the tower, and the base of the tower is fixed. The modal analysis results obtained from the present parametric FEA model with shell elements are compared against those from the ADAMS software documented in Jonkman and Bir (2010), and the comparison results are presented in Table 8.

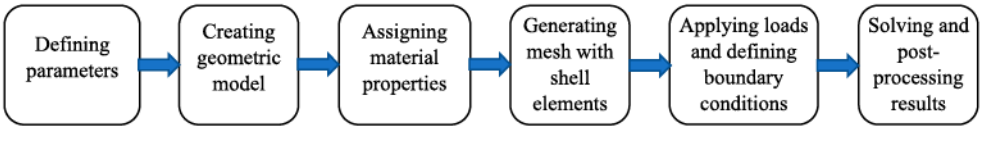

Figure 4. Flowchart of the parametric FEA model of onshore WT towers with shell elements.

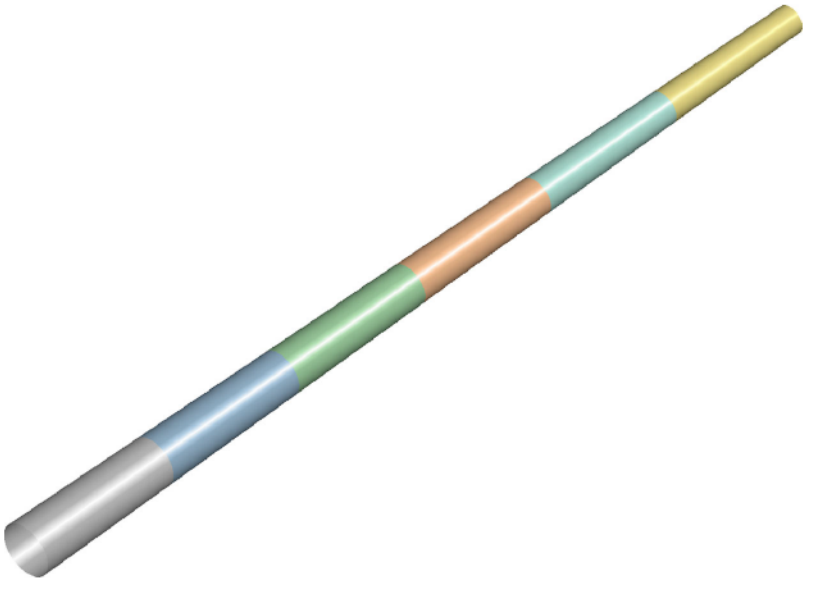

Figure 5. Geometric model of the 2.0 MW onshore WT tower.

Table 5. Material properties of S355 steel (Al-Sanad et al. 2021).

Property	Value	Unit
Density	8500	kg/m^3
Poisson's ratio	0.3	–
Young's modulus	210	GPa

As can be seen from Table 8, both fore-aft and side-to-side modal frequencies of the NREL 5MW WT tower predicted from the present FEA model with shell elements show good agreement with the those reported in Jonkman and Bir (2010), having the maximum percentage difference (1.51%) occurred at the 2nd side-to-side mode. This indicates that the present FEA model with shell elements is valid.

5. Genetic algorithm

A GA, which is a widely used search heuristic inspired by Darwin's theory of natural evolution, is taken in this work to search for optimum solutions. A population of individuals evolves in the GA toward better solutions. The evolution in the GA is an iterative process, beginning with an initial population with individuals that are randomly generated. In every iteration, the GA evaluates the fitness of each individual. Those individuals having better fitness are stochastically chosen from the present population. A new generation, which is created through recombining and

Table 6. Meshing parameters and calculated maximum deformation.

Mesh size (m)	Maximum deformation (m)	Diff (%)	Number of elements
2.5	0.197	46.5	144
2.0	0.135	7.4	336
1.5	0.125	2.5	648
1.0	0.122	2.2	1248
0.5	0.120	0.8	4368
0.25	0.119	–	18,720

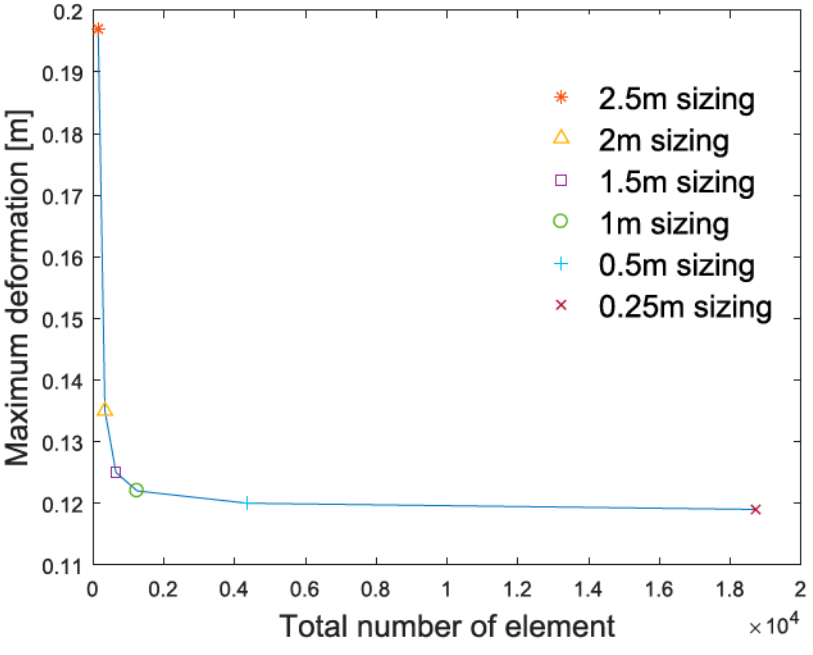

Figure 6. Meshing parameters and calculated maximum deformation.

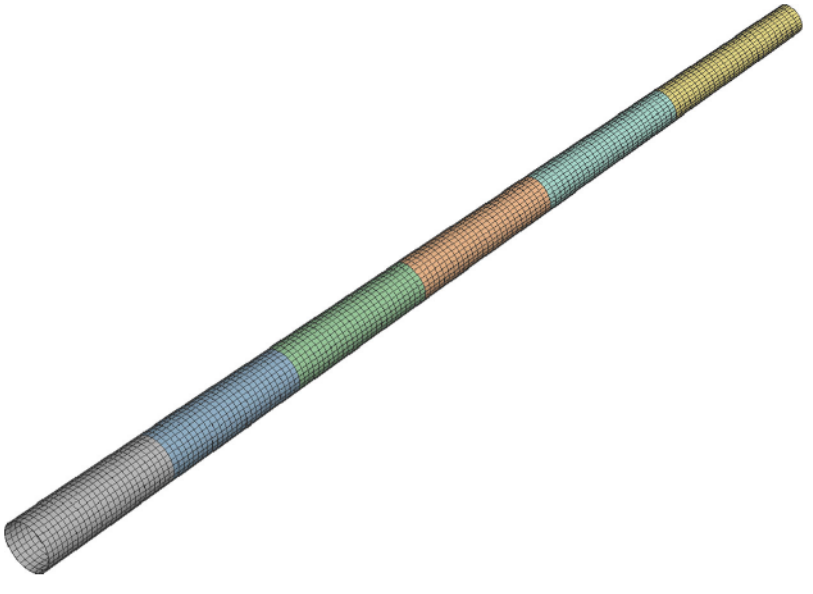

Figure 7. FEA Mesh of the 2MW WT tower with shell elements.

mutating the genome of each individual, then proceeds to the next iteration. The optimisation process of GA commonly terminates when either the maximum number of generations has been generated or a satisfactory fitness level has been reached by the present population. Further information on GA can be obtained in Kramer (2017).

The optimum solution is searched in the GA using the following procedure:

Table 7. Geometric and material properties of the NREL 5MW WT tower (Jonkman et al. 2009).

Item	Value	Unit
Tower base diameter	6	m
Tower top diameter	3.87	m
Tower base thickness	0.0351	m
Tower top thickness	0.0247	m
Density	8500	kg/m^3
Shear modulus	80.8	GPa
Young's modulus	210	GPa
RNA mass	350,000	kg

Table 8. Modal analysis results of the NREL 5MW WT tower.

Modal frequencies	Present FEA model with shell elements	ADAMS (Jonkman and Bir 2010)	% Diff
1st side-to-side (Hz)	0.3173	0.3188	0.47
1st fore-aft (Hz)	0.3202	0.3218	0.49
2nd side-to-side (Hz)	1.8542	1.8820	1.48
2nd fore-aft (Hz)	2.2054	2.2391	1.51

(1) Defining objectives, variables and constraints: in this step, the optimisation objectives, design variables and design constraints involved in the optimisation problem are defined;
(2) Generating initial population: the initial population (candidate solutions) is created randomly across the search space in this step;
(3) Producing a new population: in this step, a new population is produced through mutation and crossover operators;
(4) Updating design points: the design points in the new population are updated in this step;
(5) Validating convergence: if the convergence criteria are met, the optimisation converges; otherwise, the optimisation process move on to the next step;
(6) validating stopping criterion: when the maximum number of iterations is reached, the optimisation process terminates; otherwise, it goes back to Step 3 to create a new population.

Steps 3 through 6 in the GA are repeated sequentially until the stopping criterion has been met or the optimisation has converged. Figure 8 presents the flowchart of the GA.

6. Structural optimisation framework for onshore WT towers

6.1. Objective function

The mass reduction of an onshore WT tower corresponds to the reduction of material cost and hence achieving economic and profitable operation of onshore WTs, while maintaining safety requirements. In this study, the minimisation of mass of the onshore WT tower, m_t, is taken as the objective function, F_{obj}. This can be expressed as:

$$F_{\text{obj}} = \min(m_t) \tag{4}$$

6.2. Design variables

The schematic of the tower structures is presented in Figure 9. It should be noticed that the length and number of the tower segments can be varied according to different assembly and manufacturing requirements. In this study, the tower structure is divided into six 13 m-length segments, as depicted in Figure 9. The tower diameter is assumed to be linearly increased from the top to the bottom. For this optimisation problem, the thickness of each tower segment as well as the bottom and top diameters of the tower are chosen as design variables. Therefore, eight design variables in

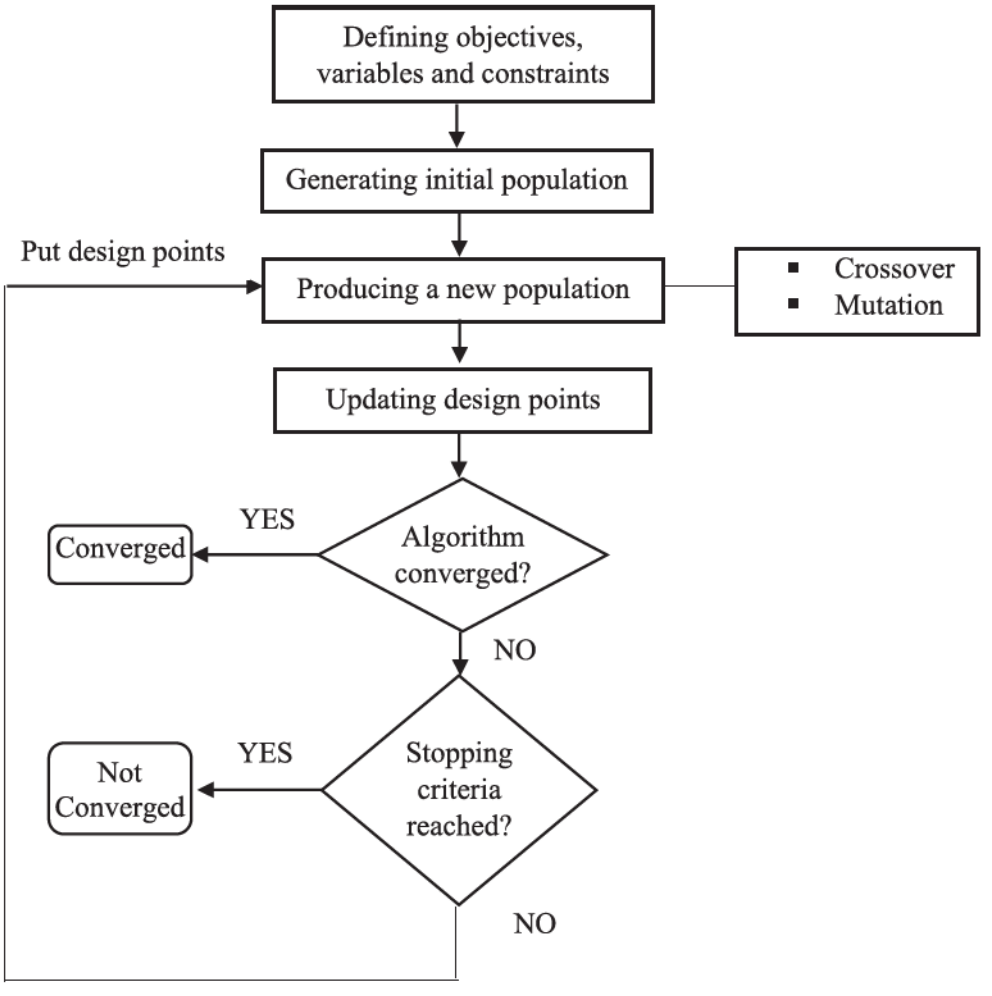

Figure 8. Flowchart of GA.

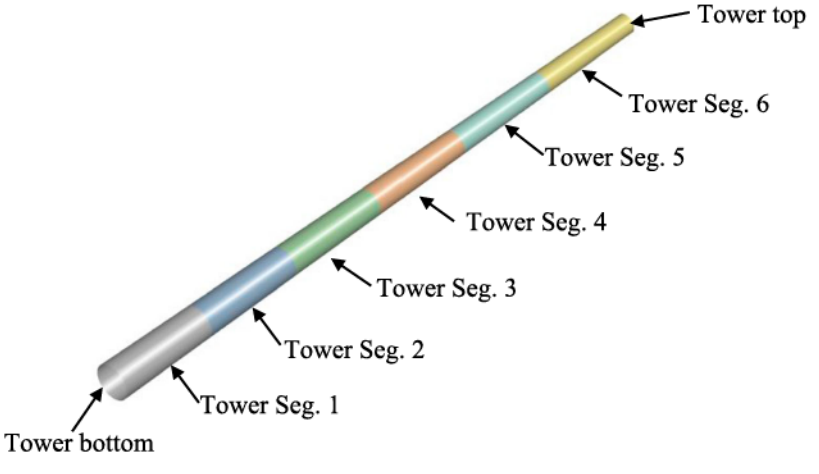

Figure 9. Schematic of tower structure and associated variables.

total are defined, which can be expressed as:

$$X = [x_1\ x_2\ \cdots\ x_n]^T,\ n = 8 \tag{5}$$

where x_1 and x_2 are the diameters of the tower top and tower bottom, respectively; x_3 to x_8 are the thicknesses of 1st to 6th tower segment, respectively.

6.3. Design constraints

6.3.1. Ultimate strength constraint

For ultimate limit state, the von-Mises stress σ should stand below the allowable stress σ_{allow}. This constraint can be expressed as:

$$\sigma \leq \sigma_{\text{allow}} \tag{6}$$

The allowable stress σ_{allow} can be calculated by:

$$\sigma_{\text{allow}} = \sigma_y / \gamma_m \tag{7}$$

where σ_y is the yield strength, with a typical value of 355 MPa for steel S355; γ_m is the material safety factor, with a value of 1.1 suggested by IEC 61400–1 (IEC 2005). Thus, the allowable stress σ_{allow} in this case is 323 MPa.

6.3.2. Maximum tower top rotation constraint

To ensure the overall stability of the onshore WT tower structure and avoid the anomalies caused by large deflections, the maximum tower top rotation θ_{max} should stand below the allowable rotation σ_{allow}. This constraint can be expressed as:

$$\theta_{\text{max}} \leq \theta_{\text{allow}} \tag{8}$$

In this study, the value of the allowable tower top rotation σ_{allow} is 5°, taken from Nicholson (2011).

6.3.3. Fatigue constraint

For structures subject to considerable cyclic loads, the fatigue is a particularly important phenomenon. During the operation of a WT, each rotation of the rotor blades can lead to stress variations in the tower structure. Besides, the availability of the WT indicates whether the rotor is under operation. The design life number of cycles N_{life} can be computed based on the rated rotor speed n_{rated} and the availability η_a (98.5%) on the selected site. For instance, assuming the service life time of the tower is 20 years, the design life number of cycles N_{life} can be calculated by:

$$N_{\text{life}} = \eta_a \times n_{\text{rated}} \times (20\ [\text{year}] \times 365[\text{day/year}] \times 24[\text{hour/day}] \times 60[\text{min/hour}]) \tag{9}$$

Following the DEL approach employed in this study, the computational cost is reduced to an equivalent load case in which an equivalent S-N curve is utilised to derive the number of cycles to failure N_{DEL}. An appropriate S-N curve of intercept $A = 13.93$ and slope $m = 4$ suggested by LaNier (2005) is taken in this study. The design life number of cycles N_{life}, which is derived from Equation (9), can be then utilised in the S-N curve to obtain the design fatigue stress range $\sigma_{f,\,\text{design}}$. The FEA simulations are used to compute the maximum fatigue stress range $\sigma_{f,\,\text{max}}$ on the tower structure. The design fatigue stress range $\sigma_{f,\,\text{design}}$ divided by the maximum fatigue stress range $\sigma_{f,\,\text{max}}$ yields the minimum fatigue safety ratio $f_{sr,\,min}$, which should not exceed the allowable fatigue safety ratio $f_{sr,\,\text{allow}}$. This constraint can be expressed as:

$$f_{sr,\text{min}} \geq f_{sr,\,\text{allow}} \tag{10}$$

The allowable fatigue safety ratio equals to one time the material safety factor for fatigue $\gamma_{m,f}$. As suggested by IEC 61400–1 (IEC 2005), the material safety factor for fatigue, $\gamma_{m,f}$, should not be less than 1.1. In this study, 1.1 is taken for $\gamma_{m,f}$, and therefore $f_{sr,\,\text{allow}}$ equals to 1.1.

6.3.4. Vibration constraint

When the 1st mode natural frequency of the WT tower, f_{1st}, is close to the rotating rotor induced frequency f_{1P} and the blade-passing frequency f_{3P}, resonance occurs, leading to significant vibration. To avoid the resonance-induced vibration, f_{1st} needs to be sufficiently separated from $f_{1P}f_{3P}$. The soft-stiff structural design, in which f_{1st} is designed to sit between the f_{1P} and f_{3P} frequencies, is presently the most economical design for WT towers. Considering tolerance of $\pm 5\%$ (Lloyd and Hamburg 2010), this constraint can be expressed as:

$$f_{1P+5\%} \leq f_{1st} \leq f_{3P-5\%} \tag{11}$$

The cut-in and rated rotor speeds of the considered 2.0 MW WT are equal to 9 and 19 rpm, respectively. Therefore, the vibration constraint can be expressed as:

$$0.333\,\text{Hz} \leq f_{1st} \leq 0.429\,\text{Hz} \tag{12}$$

6.3.5. Buckling constraint

Thin-walled structures, such as WT towers, are prone to experience buckling failure. The critical load divided by the currently applied load gives the buckling load multiplier L_m, which should stand above the allowable load multiplier $L_{m,\text{allow}}$ to avoid the buckling failure. This constraint can be expressed as:

$$L_m \geq L_{m,\,\text{allow}} \tag{13}$$

The allowable load multiplier $L_{m,\text{allow}}$ used in this study is equal to 1.4, taken from DNV GL (2016).

6.3.6. Design variable constraint

In order to ensure a realistic and feasible WT tower design, each design variable is restricted to change within a predefined range through the following constraint:

$$x_i^L \leq x_i \leq x_i^U \; i = 1,\; 2,\; \cdots,\; 8 \tag{14}$$

where x_i^L and x_i^U are the lower and upper bounds of the design variables, respectively.

The resultant loads on the WT tower bottom are normally greater than those on the tower top, and therefore larger diameter is required at the tower bottom to resist the greater resultant loads. To ensure the tower bottom diameter is greater than the tower top diameter, the following constraint is used:

$$x_2 - x_1 \geq 0 \tag{15}$$

Additionally, the thickness of the WT tower normally increases from the tower top to the tower bottom. In order to ensure this, the following constraint is added:

$$x_i - x_{i-1} \geq 0 \; i = 4,\; 5,\; \cdots,\; 8 \tag{16}$$

The bounds of constraint conditions and design variables utilised in the structural optimisation of onshore WT towers are summarised in Table 9.

Table 9. Bounds of constraint conditions and design variables.

Item	Lower bound	Upper bound	Unit	Definition
σ	–	323	MPa	von-Mises stress
θ_{max}	–	5	Degree	Maximum tower top rotation
$f_{sr,min}$	1.1	–	–	Fatigue safety ratio
f_{1st}	0.333	0.429	Hz	Tower first natural frequency
L_m	1.4	–	–	Buckling load multiplier
x_1	1.5	4	m	Tower top diameter
x_2	3.5	5.5	m	Tower bottom diameter
$x_3 \sim x_8$	0.015	0.045	m	Thickness of tower segments

6.4. Parameters setting in the GA

The GA illustrated in Section 5 is employed to find optimum solutions in the optimisation problem. The major parameters utilised in the GA are summarised in Table 10 and are further explained in this section.

- Type of initial sampling

The initial samples (i.e. the initial population) are created using a constrained sampling algorithm, ensuring the satisfaction of Equations (14)–(16).

- Number of initial samples

The number of initial samples N_{Ini}, also known as initial population size, is an important parameter that affects the ability of the GA to search an optimum solution in the search space. Its minimum value needs to be no less than ten times the number of design variables. In this study, in order to enlarge the probability of achieving a better solution, the number of initial samples N_{Ini} is set to 100, which is 12.5 times the number of design variables.

- Number of samples per iteration

The convergence speed of the optimisation can be affected by the number of samples per iteration N_{PerIter}, for which an empirical value of 40 is used in this work.

- Maximum number of iterations

The iteration of GA terminates when the maximum number of iterations N_{MaxIter} is reached. This number (30 in this study) together with the number of initial samples N_{Ini} and number of samples per iteration N_{PerIter} yields the maximum number of evaluations N_{MaxEval}, which can be

Table 10. Major parameters utilised in the GA.

Item	Value
Type of initial sampling	Constrained sampling
Number of initial samples N_{Ini}	100
Number of samples per iteration N_{PerIter}	40
Maximum number of iteration N_{MaxIter}	30
Mutation probability	0.01
Crossover probability	0.82
Maximum allowable Pareto percentage (%)	70
Convergence stability percentage (%)	2

expressed:

$$N_{\mathrm{MaxEval}} = N_{\mathrm{Ini}} + N_{\mathrm{PerIter}} \times (N_{\mathrm{MaxIter}} - 1) \tag{17}$$

- Mutation probability

The mutation probability, which determines how many chromosomes should be mutated in each generation, has a value in the range between 0 and 1. This probability should be set low. When the value of the mutation probability is equal to 1, the search in the GA will turn into a primitive random search. In this study, a typical value of 0.01 (Perez, Chung, and Behdinan 2000) used for this probability.

- Crossover probability

The crossover probability, of which value lies between 0 and 1, determines the number of times that a crossover occurs for chromosomes in each generation. If the value of the crossover probability is equal to 1, it means that all offspring are made by crossover. If it is equal to 0, then the new generation of individuals are copied exactly from their parents (i.e. older population), except those created from the process of the mutation. In this study, A typical value of 0.82 (Gandomkar, Vakilian, and Ehsan 2005) is used for this probability.

- Maximum allowable Pareto percentage

The number of desired Pareto points divided by the number of samples per iteration gives the Pareto percentage, which here stands as the convergence criterion. When the Pareto percentage researches the maximum allowable value (70% in this study), the optimisation converges.

6.4.1. Convergence stability percentage

The convergence criterion is derived on the basis of mean, standard deviation and maximum spread of the output parameters. When this criterion value reaches 2.0%, the optimisation is deemed as converged in this study.

6.5. Flowchart of optimisation framework

Figure 10 depicts the flowchart of the structural optimisation framework for onshore WT towers, which combines the parametric FEA model (illustrated in Section 4) with the GA (illustrated in Section 5).

7. Results and discussion

7.1. Evolution of WT tower mass

Figure 11 presents the evolutionary history of the WT tower mass. From Figure 11, we can see that the mass of the WT tower reduces gradually with the evolution, reaching the best design with a mass of 172 tons after 520 evaluations. An outcome of 13.5% of mass saving, corresponding to an absolute mass reduction of 27 tons, is achieved in the optimal design when compared to the initial design with a mass of 199 tons.

7.2. Design constraints

Figures 12–16 present the history of maximum von-Mises stress, maximum tower top rotation, fatigue safety ratio, 1st mode natural frequency and buckling load multiplier of the WT tower,

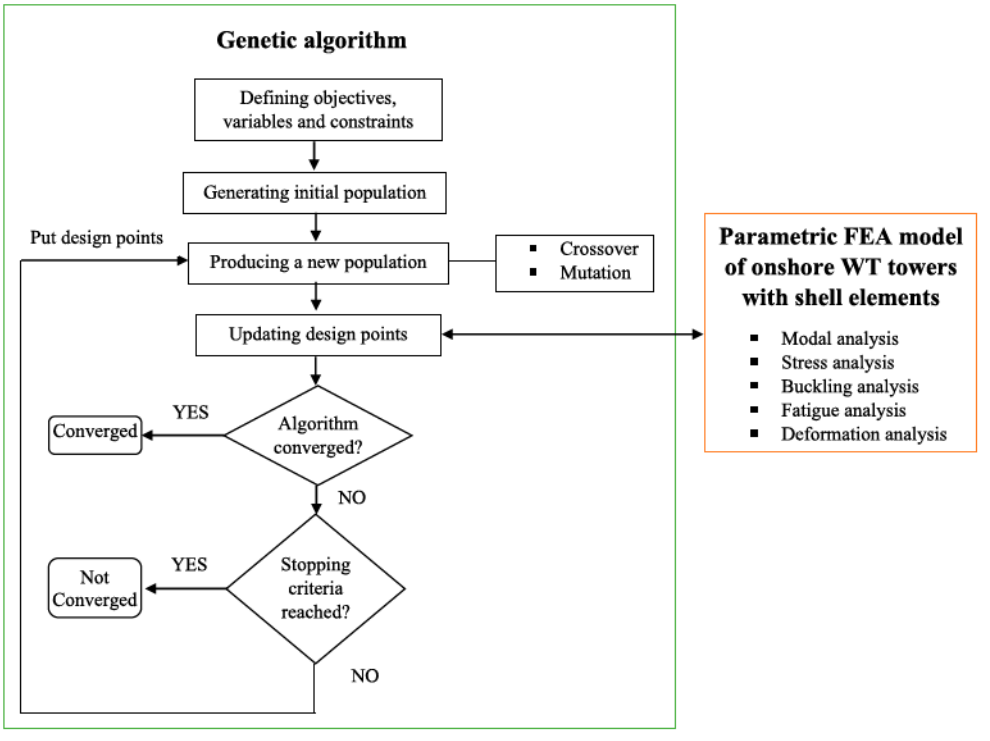

Figure 10. Flowchart of structural optimisation framework for onshore WT towers.

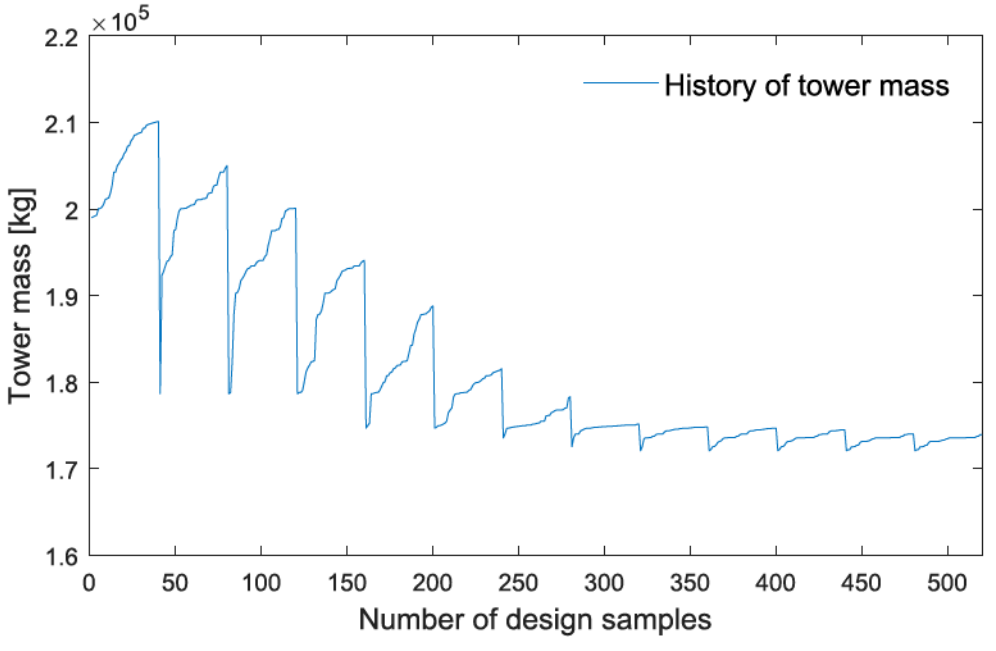

Figure 11. History of WT tower mass.

respectively. To facilitate the illustration, the associated allowable values (i.e. lower or upper bounds) are included in these figures as well. From Figures 12–16, we can see that the design is predominantly driven by the fatigue safety ratio, which appears to be the most saturated design constraint.

7.3. Design variables

The optimal value of the design variables is summarised in Table 11. From Table 11, we can see that the optimal value of all design variables satisfies design variable constraints defined in Equations (14)–(16).

7.4. Structural results of the optimal design

The deformation, von-Mises stress distribution, buckling and modal frequencies analysis results of the optimal design are illustrated and discussed below.

7.4.1. Deformation

Figure 17 depicts the deformations of the optimal WT tower under the ultimate load case. From Figure 17, we can see that the maximum deformation is around 1.53 m, occurring at the top of the tower. The maximum tower top rotation is 2.51°, which stands below the allowable value of 5°. This indicates that it is unlikely for the optimal tower design to experience large tower top rotation.

7.4.2. von-Mises stress distribution

Figure 18 presents the von-Mises stress distributions of the optimal WT tower under the ultimate load case. From Figure 18, we can see that the maximum von-Mises stress is around 224 MPa, which is 30.6% smaller than the allowable value of 323 MPa. This means that the optimal tower design is safe under ultimate limit state.

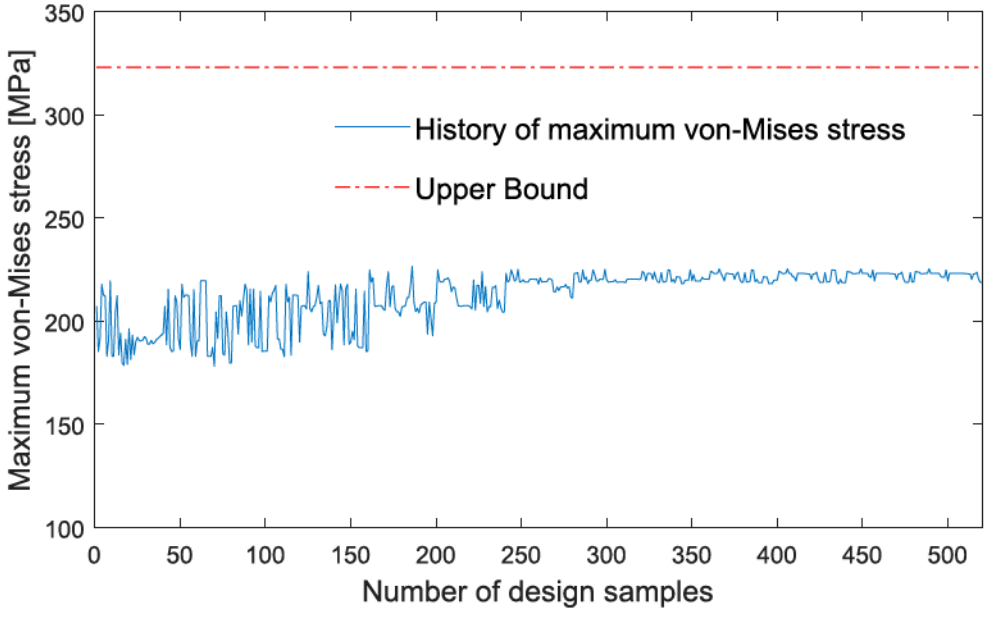

Figure 12. History of maximum von-Mises stress within the WT tower structure for ultimate load case.

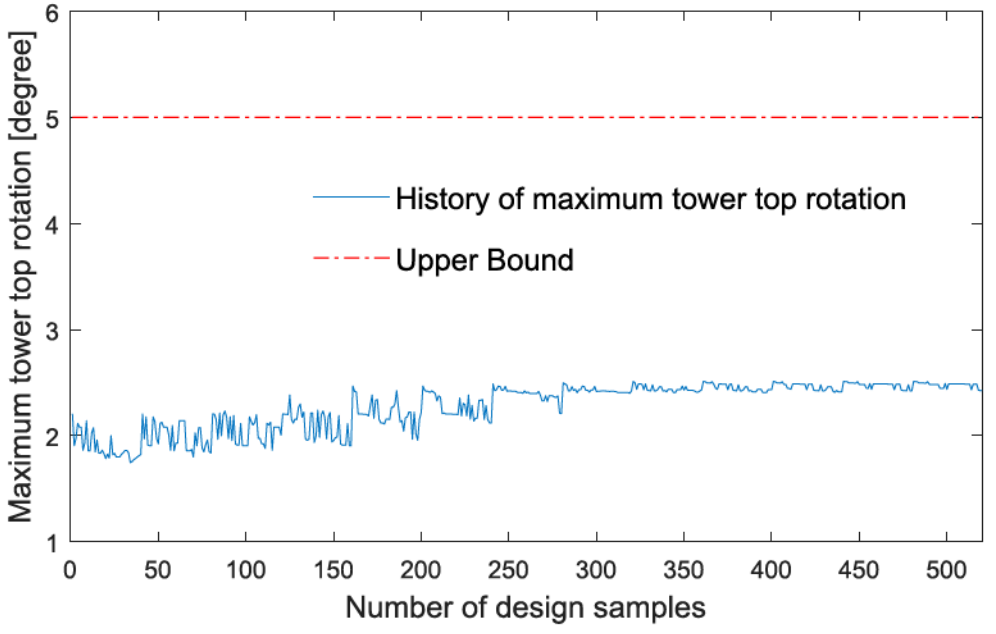

Figure 13. History of maximum tower top rotation for ultimate load case.

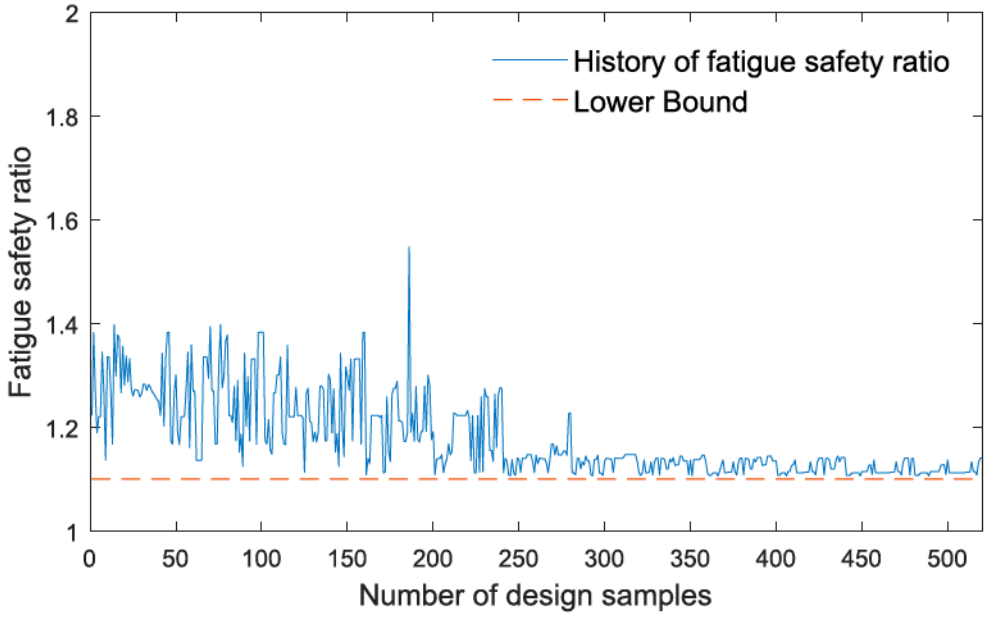

Figure 14. History of fatigue safety ratio for fatigue load case.

7.4.3. Buckling

Figure 19 presents the buckling analysis results of the optimal WT tower. From Figure 19, we can see that the buckling load multiplier is around 8.18, which is well above the minimum acceptable value of 1.4. This indicates that it is unlikely for the optimal tower design to suffer from buckling failure.

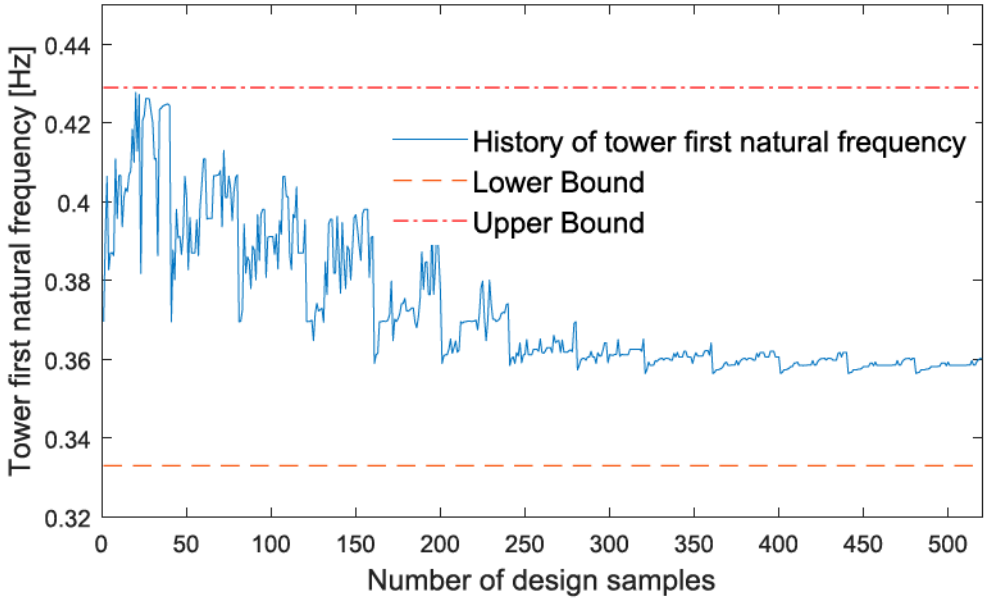

Figure 15. History of 1st mode natural frequency of the WT tower.

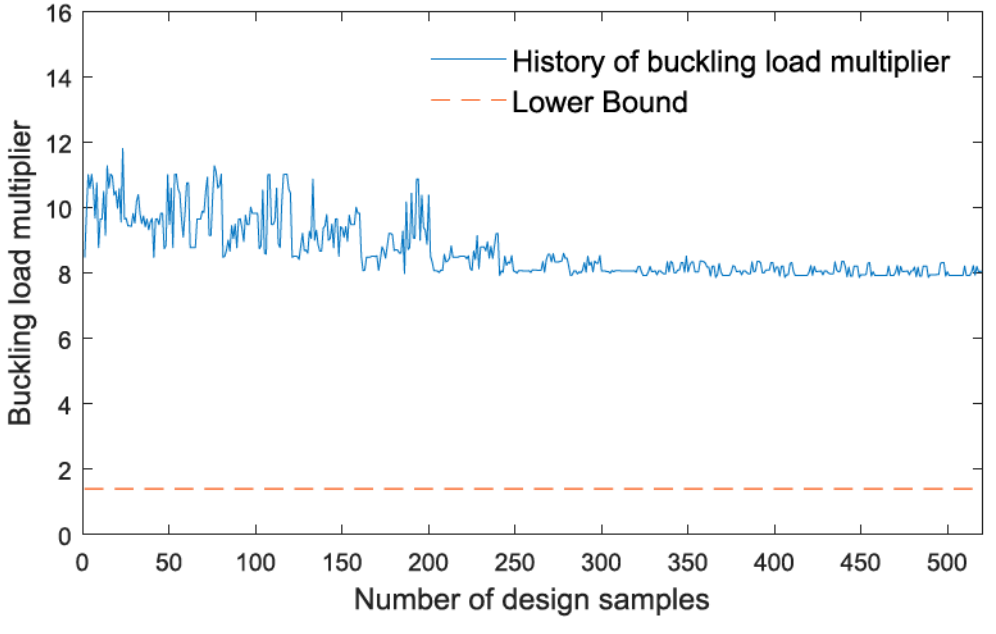

Figure 16. History of buckling load multiplier for ultimate load case.

7.4.4. Modal frequencies and shapes

Figure 20 depicts the 1st mode modal shape and natural frequency of the optimal WT tower. From Figure 20, we can see that the 1st mode natural frequency is around 0.356 Hz, which lies between the desired range of 0.333 and 0.429 Hz. This indicates that the optimal WT tower design is unlikely to suffer from resonance-induced vibration.

Table 11. Optimal value of design variables.

Design variable	Optimal value (m)	Definition of variable
x_1	2.158	Tower top diameter
x_2	4.297	Tower bottom diameter
	0.032	Segment 1 thickness
x_4	0.029	Segment 2 thickness
x_5	0.026	Segment 3 thickness
x_6	0.023	Segment 4 thickness
x_7	0.020	Segment 5 thickness
x_8	0.017	Segment 6 thickness

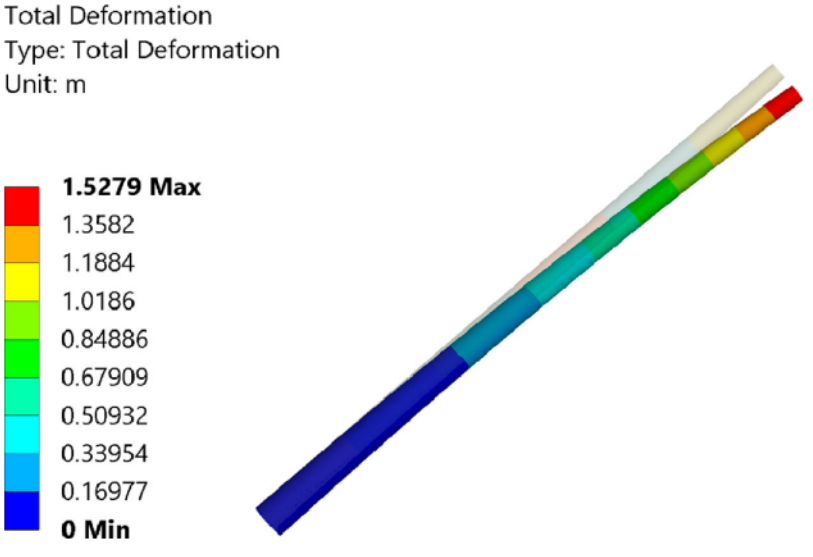

Figure 17. Deformation of optimal WT tower.

Figure 18. von-Mises stress distributions of the optimal WT tower.

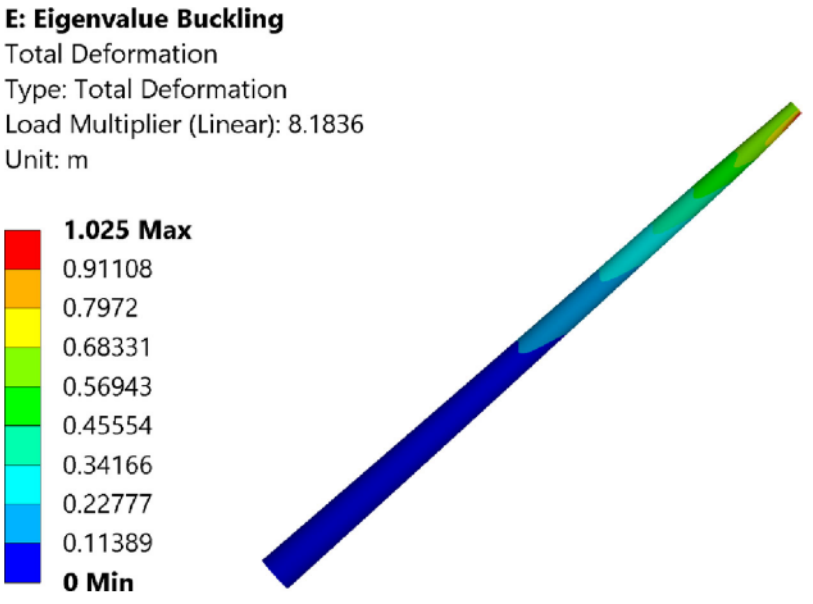

Figure 19. Buckling mode shape of optimal WT tower.

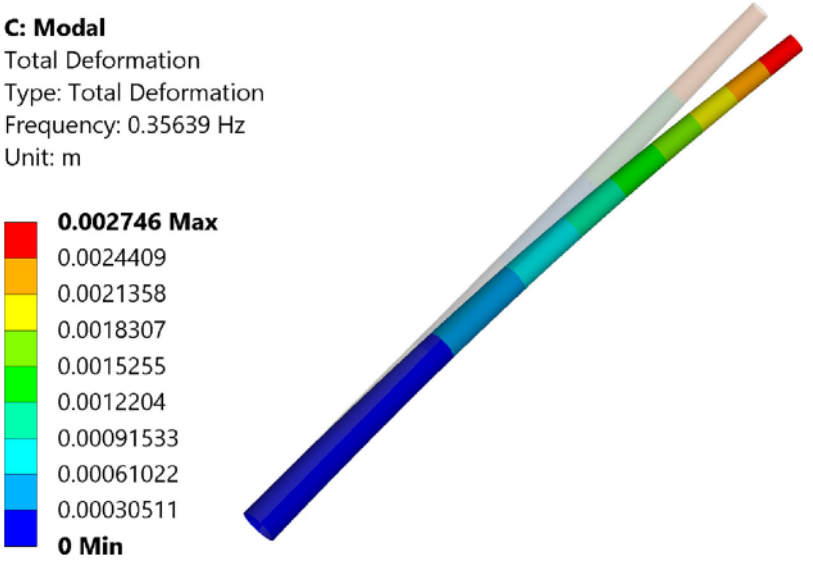

Figure 20. 1st mode modal shape and natural frequency of the optimal WT tower.

7. Conclusions

By integrating a parametric finite element analysis (FEA) model with a genetic algorithm (GA), a structural optimisation framework for onshore wind turbine (WT) towers considering multiple design constraints has been developed in this work. The onshore WT tower mass is minimised by the structural optimisation framework with multiple constraint conditions, i.e. ultimate strength, tower top rotation, vibration, buckling, fatigue and design variable constraints. The bottom and top diameters of the tower as well as the thicknesses of tower segments are chosen as the design variables. The structural optimisation framework developed in this work has been made an application

to a representative 2.0 MW onshore WT tower. From the present study, the following main conclusions can be obtained:

- The modal analysis results from the present FEA model of WT towers with shell elements show good agreement with the values documented in the literature, having a maximum percentage difference of 1.51%. This proves the validity of the present FEA model with shell elements.
- In comparison to the initial tower design, the optimal tower design achieves a mass reduction of 13.5%, which indicates that the mass of the onshore WT tower can be considerably reduced while fulfilling design constraints, leading to a more cost-effective structure.
- The tower design in the present case is predominantly driven by the fatigue safety ratio, which appears to be the most saturated design constraint.
- The structural optimisation framework for onshore WT towers can effectively and accurately determine the optimal diameters and thickness distributions of onshore WT towers, and has the potential to considerably improves structural design of onshore WT towers.

Moreover, the optimisation framework developed in this work is generic in nature, and it is applicable to a number of relevant problems, optimising engineering structures and systems subject to multiple design constraints.

Disclosure statement

No potential conflict of interest was reported by the author(s).

ORCID

Athanasios Kolios http://orcid.org/0000-0001-6711-641X

References

Al-Sanad, S., L. Wang, J. Parol, and A. Kolios. 2021. "Reliability-Based Design Optimisation Framework for Wind Turbine Towers." *Renewable Energy* 167: 942–953.

Angus, D., and C. Woodward. 2009. "Multiple Objective Ant Colony Optimisation." *Swarm Intelligence* 3 (1): 69–85.

ANSYS. 2015. ANSYS Help Documentation, ANSYS, Inc. Theory Release 8.

Bir, G., and P. Migliore. 2004. *Preliminary Structural Design of Composite Blades for Two- and Three-Blade Rotors*. Golden, CO: National Renewable Energy Lab.

Cox, K., and A. Echtermeyer. 2012. "Structural Design and Analysis of a 10MW Wind Turbine Blade." *Energy Procedia* 24: 194–201.

DNV GL. 2016. *DNVGL-ST-0126: Support Structures for Wind Turbines*. Oslo: DNV GL.

Freebury, G., and W. Musial. 2000. "Determining Equivalent Damage Loading for Full-Scale Wind Turbine Blade Fatigue Tests." *2000 ASME Wind Energy Symposium*, 50, Reno, Nevada, USA.

Fried, L., S. Shukla, S. Sawyer, and S. Teske. 2016. *Global Wind Outlook 2016*.

Gandomkar, M., M. Vakilian, and M. Ehsan. 2005. "A Combination of Genetic Algorithm and Simulated Annealing for Optimal DG Allocation in Distribution Networks." In *Canadian Conference on Electrical and Computer Engineering*, 645–648. IEEE, Saskatoon, Saskatchewan, Canada.

Gentils, T., L. Wang, and A. Kolios. 2017. "Integrated Structural Optimisation of Offshore Wind Turbine Support Structures Based on Finite Element Analysis and Genetic Algorithm." *Applied Energy* 199: 187–204.

IEC. 2005. IEC 61400-1, Wind Turbines – Part 1.

Jonkman, J., and G. Bir. 2010. *Recent Analysis Code Development at NREL*. Albuquerque, New Mexico, USA: NREL (National Renewable Energy Laboratory).

Jonkman, J., S. Butterfield, W. Musial, and G. Scott. 2009. *Definition of a 5-MW Reference Wind Turbine for Offshore System Development*. Golden, CO: National Renewable Energy Lab. (NREL).

Joshi, D., K. Sandhu, and R. Bansal. 2013. "Steady-state Analysis of Self-Excited Induction Generators Using Genetic Algorithm Approach Under Different Operating Modes." *International Journal of Sustainable Energy* 32 (4): 244–258.

Kituu, G. M., D. Shitanda, C. Kanali, J. Mailutha, and J. Wainaina. 2012. "Artificial Breeding of an Optimized Solar Tunnel Dryer Using Genetic Algorithms." *International Journal of Sustainable Energy* 31 (5): 313–325.

Kolios, A., L. Wang, A. Mehmanparast, and F. Brennan. 2019. "Determination of Stress Concentration Factors in Offshore Wind Welded Structures Through a Hybrid Experimental and Numerical Approach." *Ocean Engineering* 178: 38–47.

Kramer, O. 2017. "Genetic Algorithms." *Genetic Algorithm Essentials*. Springer, 11–19.

LaNier, M. W. 2005. *LWST Phase I Project Conceptual Design Study: Evaluation of Design and Construction Approaches for Economical Hybrid Steel/Concrete Wind Turbine Towers; June 28, 2002–July 31, 2004*. Golden, CO: National Renewable Energy Lab.

Lloyd, G., and G. Hamburg. 2010. *Guideline for the Certification of Wind Turbines*.

Martinez-Luengo, M., A. Kolios, and L. Wang. 2017. "Parametric FEA Modelling of Offshore Wind Turbine Support Structures: Towards Scaling-up and CAPEX Reduction." *International Journal of Marine Energy* 19: 16–31.

Mellit, A. 2008. "Sizing of Stand-Alone Photovoltaic Power Supply System Based on Genetic Algorithm and Neuro-Fuzzy: Application for Isolated Areas." *International Journal of Sustainable Energy* 27 (2): 49–60.

Murtagh, P., B. Basu, and B. Broderick. 2004. "Simple Models for Natural Frequencies and Mode Shapes of Towers Supporting Utilities." *Computers & Structures* 82 (20–21): 1745–1750.

Nicholson, J. C. 2011. *Design of Wind Turbine Tower and Foundation Systems: Optimization Approach*.

Ohlenforst, K., S. Sawyer, A. Dutton, B. Backwell, R. Fiestas, J. Lee, L. Qiao, F. Zhao, and N. Balachandran. 2019. *Global Wind Report 2018 (Technical Report)*. Brussels, Belgium: Global Wind Energy Council.

Perez, R., J. Chung, and K. Behdinan. 2000. "Aircraft Conceptual Design Using Genetic Algorithms." *8th Symposium on Multidisciplinary Analysis and Optimization*, 4938, Long Beach, California, USA.

Petrini, F., S. Manenti, K. Gkoumas, and F. Bontempi. 2010. "Structural Design and Analysis of Offshore Wind Turbines from a System Point of View." *Wind Engineering* 34 (1): 85–107.

Riffi, M. E. 2020. "Elephants Herding Optimization to Solve the Multiple Travelling Salesman Problem, Advanced Intelligent Systems for Sustainable Development (AI2SD2019)." *Advanced Intelligent Systems for Applied Computing Sciences* 4: 224.

Schubel, P. J., and R. J. Crossley. 2012. "Wind Turbine Blade Design." *Energies* 5 (9): 3425–3449.

Stehly, T. J., P. Beiter, D. Heimiller, and G. Scott. 2018. 2017 Cost of Wind Energy Review (No. NREL/TP-6A20-72167).

Wang, L., A. Kolios, T. Nishino, P.-L. Delafin, and T. Bird. 2016. "Structural Optimisation of Vertical-Axis Wind Turbine Composite Blades Based on Finite Element Analysis and Genetic Algorithm." *Composite Structures* 153: 123–138.

Wang, L., X. Liu, N. Renevier, M. Stables, and G. M. Hall. 2014. "Nonlinear Aeroelastic Modelling for Wind Turbine Blades Based on Blade Element Momentum Theory and Geometrically Exact Beam Theory." *Energy* 76: 487–501.

Wang, L., R. Quant, and A. Kolios. 2016. "Fluid Structure Interaction Modelling of Horizontal-Axis Wind Turbine Blades Based on CFD and FEA." *Journal of Wind Engineering and Industrial Aerodynamics* 158: 11–25.